I&EC research
Industrial & Engineering Chemistry Research

ARTICLE

pubs.acs.org/IECR

Modeling Pt^{2+} Coordination Process within Poly(amidoamine) Dendrimers for Synthesis of Dendrimer-Encapsulated Pt Nanoparticles

Daigo Yamamoto, Satoshi Watanabe, and Minoru T. Miyahara*

Department of Chemical Engineering, Kyoto University, Katsura, Nishikyo, Kyoto 615-8510, Japan

Supporting Information

ABSTRACT: Dendrimer-encapsulated Pt nanoparticles can be synthesized by Pt^{2+} coordination with dendrimers followed by reduction. In the present study, we have systematically investigated the coordination kinetics of $PtCl_4^{2-}$ with fourth-generation hydroxyl-terminated poly(amidoamine) (PAMAM G4-OH) dendrimers using UV−vis spectroscopy measurements. Our experimental investigation clarifies that Pt^{2+} coordination with dendrimers occurs after the H_2O ligand exchange (aquation) of $PtCl_4^{2-}$ and that a resultant species $PtCl_2(H_2O)_2$ predominantly coordinates with the dendrimers. From these results, we have proposed a simple dynamic model that describes the Pt^{2+} coordination as a consecutive reaction composed of the aquation reaction of $PtCl_4^{2-}$ and a subsequent coordination reaction of the resultant $PtCl_2(H_2O)_2$ with the dendrimers. Our proposed model is in good agreement with the experimental results at a low concentration condition of $PtCl_4^{2-}$, validating its performance. Furthermore, we suggest that the proposed scheme can be generalized and applied to metal species other than Pt^{2+}.

INTRODUCTION

Dendrimers, according to Tomalia et al., are starburst polymers, which show regular branching with radial symmetry.[1] Owing to their unique structure, they can be applied in various fields such as catalysis, biotechnology, and construction of optical devices.[2] In these applications, the role of dendrimers as templates that encapsulate nanoparticles has attracted great interest because the template effect reduces the dimension of nanoparticles to less than two nanometers, and poly(amidoamine) (PAMAM) dendrimers are most popular for such applications.[3,4] The synthesis involves two processes: 1. metal ion coordination within the dendrimers and 2. reduction by a strong reducing agent, typically $NaBH_4$.[5] The coordination process leads to the formation of a coordinate bond between the metal ions and tertiary amine groups of the dendrimers. The subsequent reduction process yields encapsulated zerovalent metal nanoparticles. The method has the following four advantages over other synthetic methods: First, the method can be universally applied to various types of nanoparticles, including not only monometallic but also bimetallic and semiconductor nanoparticles.[6] Second, the size of the resultant nanoparticles can be controlled at an atomic level by changing the molar ratio between the metal ion and dendrimer. The nanoparticles are assumed to consist of the same number of atoms as the molar ratio. Especially in the case of Au, the average diameter of resultant nanoparticles agrees fairly well with the theoretical diameter by setting the ratio to magic numbers.[7] Third, the dendrimer-encapsulated nanoparticles show much higher catalytic activity than conventional catalysts because dendrimers have an open structure so that the reactants can easily penetrate the dendrimer periphery to reach the surface atoms of nanoparticles. Yamamoto et al. recently demonstrated that Pt nanoparticles encapsulated within dendrimers show over 10 times higher catalytic activity than commercial catalysts in the oxygen reduction reaction required for fuel cells.[8] In addition, the selectivity of reactants can be manipulated by changing the surface density of dendrimers.[9] Fourth, dendrimer surfaces can be modified to incorporate various types of functional groups. Fourth-generation PAMAM dendrimers terminated with hydroxyl groups (G4-OH) are commonly used in water solvents. Nanoparticles can also be prepared using PAMAM dendrimers with other surface functional groups such as $-COOCH_3$, $-NHCH_2CH(OH)CH_2N^+(CH)_3Cl^-$, $-NH_2$, $-C_{12}$, and $-COO^-$ by adjusting the pH or using organic solvents.[10−14]

The key process in the synthesis of dendrimer-encapsulated nanoparticles is the coordination process because a reduction reaction immediately after mixing metal ions and dendrimers, that is, without the coordination process, does not produce dendrimer-encapsulated nanoparticles.[15] Thus, the clarification of not only the equilibrium states but also the dynamics of the coordination process is quite important for the preparation of dendrimer-encapsulated nanoparticles. So far, the chemical equilibrium of metal ion coordination with dendrimers has been mainly investigated and is understood relatively well. Tarazona-Vasquez and Balbuena have proposed models of the ligand exchange reaction of Pt^{2+} on the basis of thermodynamics.[16−19] On the other hand, the dynamics of metal ion coordination has not been understood well. Especially in the case of Pt^{2+}, the coordination dynamics has been reported to exhibit a strange behavior. Pt^{2+} coordination within dendrimers takes a long time: in the order of days, whereas Cu^{2+} and Pd^{2+} complete their

Received: March 7, 2011
Accepted: May 16, 2011
Revised: May 11, 2011
Published: May 16, 2011

dx.doi.org/10.1021/ie200435b | Ind. Eng. Chem. Res. 2011, 50, 7332–7337

coordination in an hour.[13,20] Gu et al. have shown that more than 3 months' time is necessary to achieve equilibrium in Pt^{2+} coordination.[21] This slow coordination rate becomes faster when aged K_2PtCl_4 solution is used instead of freshly prepared precursor solutions, as demonstrated by Knecht et al.[22] Since the aging process produces several species of Pt^{2+} complexes due to H_2O ligand exchange (aquation) reactions, this result suggests that the ligands of Pt^{2+} complexes are closely related to the Pt^{2+} coordination rate. However, the key species of the complexes as well as the reaction scheme of coordination is completely unclear. In our previous study, we have demonstrated that the increase in temperature dramatically increases Pt^{2+} coordination rate, although the mechanism causing this increase is unclear.[10]

In the present study, we have explored the kinetic process of the coordination of Pt^{2+} with PAMAM dendrimers by measuring UV−vis spectra. We have examined the effects of various factors such as the aging period of Pt^{2+} ions and salt concentration. On the basis of these results, we have developed a simple model to describe the rate process of the coordination, and demonstrated the validity of the model through a comparison between the proposed model and experimental results.

EXPERIMENTAL SECTION

Chemicals. Fourth-generation, hydroxyl-terminated PAMAM dendrimers (G4-OH, 10 wt % solution in methanol), sixth-generation dendrimers (G6-OH, 5 wt % solution in methanol), and potassium tetrachloroplatinate(II) (K_2PtCl_4, 99.99%) were purchased from Aldrich Chemical Co. The G4-OH and G6-OH dendrimers were dried under vacuum at room temperature to remove the solvent prior to use. Sodium chloride (NaCl, 99.5%) was also purchased from Aldrich Chemical Co. and used as received. Ultrapure deionized (DI) water (18 MΩcm, Millipore) was used to prepare all the aqueous solutions.

Pt^{2+} Coordination. Pt^{2+} was coordinated with G4-OH dendrimers according to a previously reported method.[23] Briefly, we first prepared a 100 μM G4-OH aqueous solution, in which Cl^- concentration was adjusted by adding NaCl, as per requirement. The G4-OH and K_2PtCl_4 solutions were mixed to obtain [G4-OH + xPt^{2+}] (x = 10, 20, 30, 40, 60, 80, 100, or 120) solution. Note that K_2PtCl_4 solution was prepared just before use because the Pt^{2+} complex species change due to aquation.[24] These solutions were vigorously stirred for a few seconds. A similar experiment was conducted using G6-OH instead of G4-OH to examine the effect of dendrimers' surface density on the coordination. The time course of UV−vis absorbance spectra of the solutions was measured for several days at 25 ± 2 °C using a UV-1700 (SHIMADZU) and quartz cells with a light-path length of 1.0 cm.

RESULTS AND DISCUSSION

For quantitative analysis of the Pt^{2+} coordination process, we first investigated the dynamics of the aquation reaction of $PtCl_4^{2-}$ without dendrimers. Figure 1 shows the UV−vis absorbance spectra of a 200 μM $PtCl_4^{2-}$ solution without dendrimers for various aging periods, which has typical concentration of 5 μM [G4-OH + 40 Pt^{2+}] in our experiments with dendrimers. The peak at 216 nm, which is attributable to the ligand-to-metal charge transfer (LMCT) transition between Pt^{2+} and Cl^-,[5] decreases with time and disappears in two days. This suggests that the aquation reaction replaced Cl^- ligands

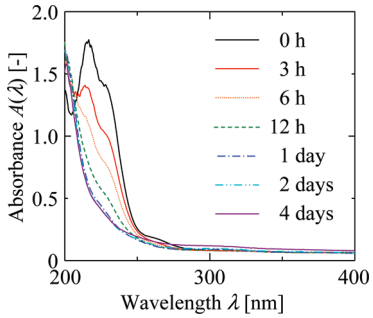

Figure 1. UV−vis absorbance spectra of a 200 μM $PtCl_4^{2-}$ solution for various aging periods without dendrimers. Air was used to obtain the background spectrum.

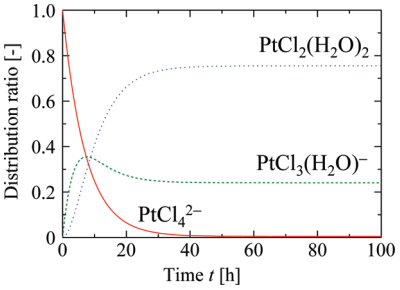

Figure 2. Calculated rate profiles of distribution ratio obtained from the aquation of $PtCl_4^{2-}$. The initial concentration was set as 200 μM and the aquation rate constants k_1 and k_3 were 0.14 h^{-1} and 0.16 h^{-1}, respectively.[24,27].

with H_2O molecules.[22,25] It has been reported that the aquation of $PtCl_4^{2-}$ produces three species of Pt^{2+} complexes [$PtCl_4^{2-}$, $PtCl_3(H_2O)^-$, and $PtCl_2(H_2O)_2$] in the K_2PtCl_4 aqueous solution.[24] Strictly speaking, other Pt^{2+} complexes such as $PtCl(H_2O)_3^+$ and $Pt(H_2O)_4^{2+}$ may also be present after aquation. However, the equilibrium constants of the aquation reaction for the two species is so small as compared to the other three that its existence can be ignored.[26] Thus, the aquation reactions of Pt^{2+} complexes at 25 °C are expressed by the following equations:[27]

$$PtCl_4^{2-} + H_2O \underset{r_2}{\overset{r_1}{\rightleftarrows}} PtCl_3(H_2O)^- + Cl^- \quad (1)$$

$$PtCl_3(H_2O)^- + H_2O \underset{r_4}{\overset{r_3}{\rightleftarrows}} PtCl_2(H_2O)_2 + Cl^- \quad (2)$$

$$r_1 = k_1[PtCl_4^{2-}] \quad (3)$$

$$r_2 = k_2[PtCl_3(H_2O)^-][Cl^-] \quad (4)$$

$$r_3 = k_3[PtCl_3(H_2O)^-] \quad (5)$$

$$r_4 = k_4[PtCl_2(H_2O)_2][Cl^-] \quad (6)$$

$$K_1 = \frac{k_1}{k_2} = \frac{[PtCl_3(H_2O)^-]_{eq}[Cl^-]_{eq}}{[PtCl_4^{2-}]_{eq}} = 1.34 \times 10^{-2}M \quad (7)$$

dx.doi.org/10.1021/ie200435b |Ind. Eng. Chem. Res. 2011, 50, 7332–7337

Table 1. Distribution Ratios at Aquation Equilibrium without Dendrimers. The Initial Concentrations of $PtCl_4^{2-}$ Correspond to Those in Figures 3 and 4[a]

$[K_2PtCl_4]_{initial}$	Pt^{2-} distributions at aquation equilibrium [%]		
	$PtCl_4^{2-}$	$PtCl_3(H_2O)^-$	$PtCl_2(H_2O)_2$
200 μM	1	24	75
300 μM	1	11	68
400 μM	2	36	62
2 mM	14	14	28
3 mM	15	63	22
4 mM	16	16	16
20 mM	45	50	5
30 mM	52	45	3
40 mM	56	41	2

[a] The ratios were obtained by solving eqs 7−10.

$$K_2 = \frac{k_3}{k_4} = \frac{[PtCl_2(H_2O)_2]_{eq}[Cl^-]_{eq}}{[PtCl_3(H_2O)^-]_{eq}} = 1.1 \times 10^{-3}\text{M} \quad (8)$$

where, k_i (i = 1−4) is the rate constant, the square brackets [ ] represent the concentration, and the subscript eq denotes the equilibrium condition.

Time course of the aquation can be calculated by using the above equations; its result is shown in Figure 2. In this calculation, we set rate constants k_1 and k_3 as 0.14 h^{-1} and 0.16 h^{-1}, respectively,[24] and the initial concentration of $PtCl_4^{2-}$ as 200 μM. The reverse reaction rate constants of the aquation reaction were obtained from the equilibrium constants K_1 and K_2 in eqs 7 and 8, respectively. The aquation takes more than 40 h to attain equilibrium, which agrees well with the time taken for the peak at 216 nm in Figure 1 to disappear. The distribution ratios of the three Pt^{2+} complexes at equilibrium were obtained by solving eqs 7 and 8, and the two following material balances of Pt^{2+} and Cl^-:

$$[K_2PtCl_4]_{initial} = [PtCl_4^{2-}]_{eq} + [PtCl_3(H_2O)^-]_{eq} + [PtCl_2(H_2O)_2]_{eq} \quad (9)$$

$$4[K_2PtCl_4]_{initial} + [NaCl]_{initial} = 4[PtCl_4^{2-}]_{eq} + 3[PtCl_3(H_2O)^-]_{eq} + 2[PtCl_2(H_2O)_2]_{eq} + [Cl^-]_{eq} \quad (10)$$

where the subscript initial denotes the initial condition. In the initial concentration (200 μM), $PtCl_2(H_2O)_2$ is predominant and the distribution ratios of $PtCl_4^{2-}$, $PtCl_3(H_2O)^-$, and $PtCl_2(H_2O)_2$ at equilibrium are 1%, 24%, and 75%, respectively. We have confirmed from calculations that the dominant species varies depending on the initial concentration of $PtCl_4^{2-}$. Briefly, $PtCl_4^{2-}$ is dominant at higher concentrations (>10 mM), whereas $PtCl_2(H_2O)_2$ is dominant at lower concentrations (<1 mM). Calculation results are summarized in Table 1.

We prepared [G4-OH + 40 Pt^{2+}] solution with various initial concentrations of K_2PtCl_4 ranging between 200 μM and 40 mM to examine the effect of the distributions of Pt^{2+} complex species on the coordination. The Pt^{2+}/G4-OH ratio x was fixed as 40. Figure 3 shows the UV−vis absorbance spectra of the solutions aged for more than 30 days. The samples with $[K_2PtCl_4]_{initial} \geq$ 400 μM were measured immediately after being diluted with DI water to set the platinum ion concentration as 200 μM. The

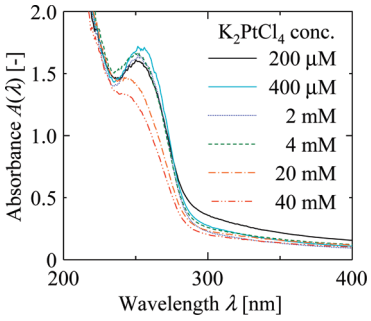

Figure 3. UV−vis spectroscopic data of [G4-OH + 40 Pt^{2+}] solutions after 30 days in the various concentrations. All samples were diluted with DI water to set the concentrations of G4-OH to 5 μM just before UV−vis measurement.

absorbance peak appeared around a wavelength of 250 nm; it is attributable to the LMCT transition between Pt^{2+} and tertiary amine sites present at the branching sites of PAMAM dendrimers.[5] The peak intensity was almost identical for the samples with concentrations ranging from 200 μM to 4 mM, among which $PtCl_2(H_2O)_2$ and $PtCl_3(H_2O)^-$ are predominant for the aquation equilibrium without dendrimers (Table 1), although several Pt^{2+}−amine group complexes $[PtCl_a(H_2O)_{4-a-b}N_b]^{2-a}$ (b = 1−4, $a + b \leq 4$) also exist.[16,17,28] It should be noted that the absorbance at 250 nm depends only on the LMCT transition between Pt^{2+} and the tertiary amines because its remains almost unchanged during the aquation reaction of $PtCl_4^{2-}$ as shown in Figure 1. Thus, it is reasonably thought that the absorption coefficients of $[PtCl_a(H_2O)_{4-a-b}N_b]^{2-a}$ (b = 1−4, $a + b \leq 4$) are similar. By introducing an average absorption coefficient $\bar{\varepsilon}$ for these Pt^{2+}−amine group complexes, the coordination ratio $\alpha(t)$, which is defined as [Pt^{2+} coordinated within dendrimers]/$[K_2PtCl_4]_{initial}$, can be estimated as follows:

$$\alpha(t) = \frac{A(t) - A(0)}{\bar{\varepsilon} l [K_2PtCl_4]_{initial}} \quad (11)$$

where, $A(t)$ is the absorbance at 250 nm at time t and l represents the light-path length of a quartz cell. $\bar{\varepsilon}$ was obtained from the slope of a spectrophotometric titration plot, which gives the relation between the ratio of Pt^{2+} per dendrimer x and the absorbance difference (See Supporting Information (SI) Figure S1). Although the definition of $\alpha(t)$ is essentially the same as that in our previous study,[10] eq 11 is extended so that it can be applied to any concentration. Another noticeable point in Figure 3 is that the absorbance around 250 nm is lower for higher concentrations (≥20 mM), where $PtCl_4^{2-}$ is predominant. This demonstrates that $PtCl_4^{2-}$ is less favorable for the coordination than $PtCl_3(H_2O)^-$ and $PtCl_2(H_2O)_2$.

To specify the key complex species of coordination, we investigated the dynamics of Pt^{2+} coordination with dendrimers for different distributions of complex species. In this experiment, Pt^{2+} ions were coordinated with G4-OH using three K_2PtCl_4 solutions, which were aged for at least 2 days in a dark room to attain aquation equilibrium. The concentrations of three K_2PtCl_4 solutions were set to be 300 μM, 3 mM, and 30 mM, in which $PtCl_2(H_2O)_2$ (68%), $PtCl_3(H_2O)^-$ (63%), and $PtCl_4^{2-}$ (52%) are respectively dominant at equilibrium (Table 1). The dendrimer concentration was 5 μM and the ratio x was set as 40, denoted as [G4-OH + 40 Pt^{2+}]. Figure 4 shows the time course of the absorbance difference at 250 nm. Coordination

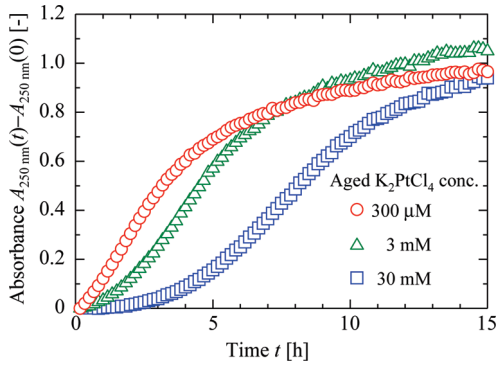

Figure 4. Time course of absorbance difference at 250 nm of 5 μM G4-OH solutions with K_2PtCl_4, which were aged for at least 2 days in various concentrations. In a 300 μM K_2PtCl_4 solution (circles), $PtCl_2(H_2O)_2$ is dominant at aquation equilibrium. In 3 mM (triangles) and 30 mM (squares) solutions, $PtCl_3(H_2O)^-$ and $PtCl_4^{2-}$ are dominant, respectively. The distributions were calculated using eqs 7 and 8 (Table 1). In all samples, the Pt^{2+} per G4-OH dendrimer ratio was fixed as 40.

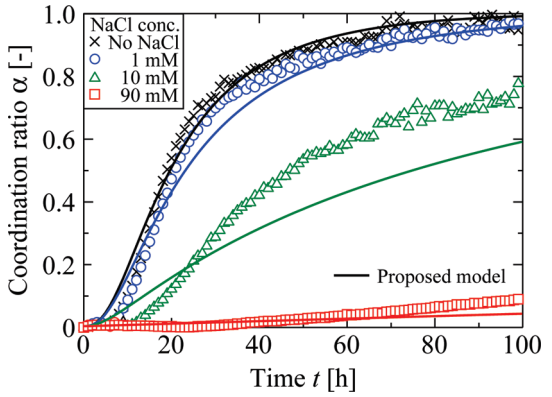

Figure 5. Time course of coordination ratio of 5 μM [G4-OH + 40 Pt^{2+}] solutions in various NaCl concentrations. Solid lines show the calculation results obtained using the proposed model. k_1, k_3, and k_5 were obtained by parameter fitting of experimental data. The values of k_1–k_5 are 1.4×10^{-1} h^{-1}, 10 M^{-1} h^{-1}, 1.6×10^{-1} h^{-1}, 1.5×10^2 M^{-1} h^{-1}, and 5.1×10^2 M^{-1} h^{-1}, respectively. Time course of the coordination ratio was calculated using the finite difference method.

Table 2. Distribution Ratios of 200 μM K_2PtCl_4 Solutions with Various NaCl Concentrations (Without Dendrimers)

$[NaCl]_{initial}$	Pt^{2+} distributions at aquation equilibrium [%]		
	$PtCl_4^{2-}$	$PtCl_3(H_2O)^-$	$PtCl_2(H_2O)_2$
no salt	1	24	75
1 mM	5	51	44
10 mM	41	54	6
90 mM	87	13	0
1M	98	2	0

Scheme 1. Proposed Model of Pt^{2+} Coordination Process within Dendrimers

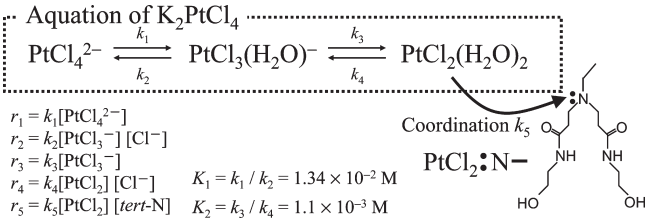

ratio α can not be determined quantitatively because a few precipitate is observed in aging K_2PtCl_4 solutions.[22] In the case of high concentrations of about 30 mM, the coordination starts after an induction period of a few hours, followed by an increase of up to 0.9 in the absorbance in 15 h. The medium concentration of about 3 mM shows a steeper initial rise in absorbance, although it still has an induction period before the coordination process. This peculiar behavior can neither be explained by the Langmuir adsorption nor by a single reaction, both of which result in an upward convex rate profile, but by a consecutive reaction. In contrast, in the case of the low concentration of 300 μM, in which $PtCl_2(H_2O)_2$ is dominant, the initial rise is rapid and the profile is similar to that of a single reaction. These results suggest that the coordination process proceeds via the aquation reaction and that $PtCl_2(H_2O)_2$ is the species that coordinates with tertiary amine groups.

To further examine the effect of the aquation process on coordination dynamics, we added NaCl to 5 μM [G4-OH + 40 Pt^{2+}] solution. Table 2 lists the equilibrium distribution ratios of a 200 μM K_2PtCl_4 solution with various NaCl concentrations. As shown in Figure 5, higher NaCl concentrations lead to slower coordination rate and longer induction periods because the addition of NaCl shifts the aquation equilibrium to the side of $PtCl_4^{2-}$ as shown in eqs 1 and 2, and increases the inverse reactions of the aquation given by eqs 4 and 6. However, it is interesting to note that the addition of NaCl did not appreciably enhance the inverse reaction of Pt^{2+} coordination. As shown in the SI Figure S2, the absorbance at 250 nm remained almost constant against the addition of excess of Cl^- to a solution, in which Pt^{2+} coordination had been completed (α = 1.0). If the coordination is a reversible reaction, Cl^- is the preferred ligand of Pt^{2+} rather than tertiary amine groups, and $PtCl_4^{2-}$ must become predominant in such high Cl^- concentrations. The Pt^{2+} coordination can thus be regarded as an irreversible reaction probably due to an extremely slow inverse reaction. The coordination bond of Pt^{2+}–tertiary amine complexes must be quite strong. This is also supported by our previous report, which demonstrated that a pH change did not decrease the coordination ratio.[10]

Modeling of Pt^{2+} Coordination Process. From the above experiments, we have demonstrated the following points:

(1) The coordination process is a consecutive reaction beginning with the aquation of $PtCl_4^{2-}$ followed by the coordination between tertiary amines and Pt^{2+} complexes, which have less Cl^-.
(2) $PtCl_2(H_2O)_2$, rather than $PtCl_4^{2-}$ and $PtCl_3(H_2O)^-$, is most likely the key species that coordinates with dendrimers.
(3) Pt^{2+} coordination can be regarded as an irreversible reaction.

Although Knecht et al. have demonstrated the point (1) qualitatively,[22] our careful experimental work makes characteristics of Pt^{2+} coordination more clear. On the basis of these results, here we have proposed a simple model of Pt^{2+} coordination (Scheme 1). The first step is the aquation of $PtCl_4^{2-}$, followed by the coordination of resultant species $PtCl_2(H_2O)_2$ with tertiary amine sites. In our model, we have assumed that only $PtCl_2(H_2O)_2$ is coordinated with tertiary amines, which

dx.doi.org/10.1021/ie200435b |Ind. Eng. Chem. Res. 2011, 50, 7332–7337

may not be correct because ^{195}Pt NMR analysis has demonstrated the existence of various types of Pt^{2+}−amine complexes.[28] However, we think that the assumption is reasonable at least in low concentrations ($[PtCl_4^{2-}]_{initial} < 1$ mM), where $PtCl_2(H_2O)_2$ is predominant as shown in Table 1. In addition, the steric hindrance against the coordination would be negligible because we confirmed that the Pt^{2+} coordination behavior into G4-OH dendrimers shows no clear difference from that into G6-OH dendrimers which have higher surface density than G4-OH (see SI Figure S3). The coordination reaction is thus described as follows:

$$PtCl_2(H_2O)_2 + tert\text{-}N^{\bullet}_{\bullet} \xrightarrow{r_5} tert\text{-}N^{\bullet}_{\bullet}PtCl_2(H_2O) + H_2O \quad (12)$$

$$r_5 = k_5[PtCl_2(H_2O)_2][tert\text{-}N^{\bullet}_{\bullet}] \quad (13)$$

where, the reaction rate is assumed to be proportional to the reactant concentrations. Note that $[tert\text{-}N^{\bullet}_{\bullet}]$ represents the concentration of the tertiary amine groups of dendrimers and is 62 times larger than [G4-OH] because a G4-OH dendrimer molecule has 62 tertiary amine groups.

Following the above coordination scheme, we calculated the time evolution of the concentrations by solving simultaneous differential equations using the finite difference method:

$$\frac{d[PtCl_4^{2-}]}{dt} = -r_1 + r_2 \quad (14)$$

$$\frac{d[PtCl_3(H_2O)^-]}{dt} = r_1 - r_2 - r_3 + r_4 \quad (15)$$

$$\frac{d[PtCl_2(H_2O)_2]}{dt} = r_3 - r_4 - r_5 \quad (16)$$

$$\frac{d[tert\text{-}N^{\bullet}_{\bullet}]}{dt} = -r_5 \quad (17)$$

$$\frac{d[tert\text{-}N^{\bullet}_{\bullet}PtCl_2(H_2O)]}{dt} = r_5 \quad (18)$$

$$\frac{d[Cl^-]}{dt} = r_1 - r_2 + r_3 - r_4 \quad (19)$$

We thereby obtained the coordination ratio $\alpha(t)$ as $[tert\text{-}N^{\bullet}_{\bullet}PtCl_2(H_2O)]/[PtCl_4^{2-}]_{initial}$. Two rate constants k_1 and k_3 we used were obtained from the work by Grantham et al.[24] and the reverse constants k_2 and k_4 were calculated from eqs 7 and 8. k_5 was obtained from fitting of the experimental data without NaCl (crosses) in Figure 5 because they would respond more sensitively to k_5 than those with NaCl. The rate constants (k_1−k_5) in the present study were 1.4×10^{-1} h^{-1}, 10 M^{-1} h^{-1}, 1.6×10^{-1} h^{-1}, 1.5×10^{2} M^{-1} h^{-1}, and 5.1×10^{2} M^{-1} h^{-1}, respectively. By using these rate constants, we calculated rate profiles for various NaCl concentrations, which are shown in Figure 5 as solid lines. The calculation results for the 1 mM NaCl agreed fairly well with the experimental results. In contrast, the calculation result for the 10 mM NaCl showed certain disagreement with the experimental data, which would be attributable to the assumption that only $PtCl_2(H_2O)_2$ is coordinated with dendrimers. The coordination between dendrimers and $PtCl_3(H_2O)^-$ can not be neglected for higher NaCl concentrations because $PtCl_4^{2-}$ and $PtCl_3(H_2O)^-$ become predominant at the aquation equilibrium as shown in Table 2. Our proposed model is applicable at lower concentration conditions of K_2PtCl_4 and NaCl, where $PtCl_2(H_2O)_2$ is predominant. However, we emphasize that the model follows the experimental trend with only one parameter (k_5), demonstrating the validity of the proposed scheme. In addition, our proposed scheme can qualitatively explain the temperature dependence of the coordination rate, which was observed in our previous study.[10] Since the difference of a few degrees in temperature can lead to a dramatic change in aquation rate constants,[24] the increase in temperature would accelerate the aquation, resulting in a shorter induction period and accordingly, faster coordination.

Table 3. Summary of Relative Kinetics of Aquation and Period of Coordination Process Within PAMAM Dendrimers for a Variety of Metal Ions

Metal species	Aquation rate[29]	Precursor	Dendrimer	Period of coordination process	ref.
Cu^{2+}	Fast	$CuSO_4$	G4-OH	Not described	20
Cd^{2+}		$Cd(NO_3)_2$	G2-OH	<30 min	30
Zn^{2+}		$Zn(NO_3)_2$	G2-OH	<30 min	30
Pd^{2+}		K_2PdCl_4	G4-OH	<1 h	13
Pt^{2+}		K_2PtCl_4	G4-OH	2 days	32
Ru^{3+}		$RuCl_3$	G4-OH	3 days	33
Ir^{3+}	Slow	$IrCl_3{\cdot}3H_2O$	G4-OH	7 days	31

Interestingly, the consecutive reaction scheme of aquation and subsequent coordination may be applicable to other metal ions. Table 3 lists the relative kinetics of the aquation and coordination periods for a variety of metal ions,[13,20,29−33] where the relative aquation rates were estimated from Figure 1 of ref 29. It is confirmed from Table 3 that a metal ion with a slower aquation rate needs a longer coordination period, demonstrating a close relation between the aquation and coordination rates, and the qualitative universality of the consecutive reaction scheme for application to various metal ions. This in turn demonstrates that periods required for the coordination process of any metal ion can be estimated only by values of aquation rate constants.

CONCLUSIONS

We investigated the rate process of Pt^{2+} coordination within PAMAM G4-OH dendrimers by measuring UV−vis absorbance spectra. On examining the effects of K_2PtCl_4 aging and NaCl addition, we found that the aquation of $PtCl_4^{2-}$ serves as an induction process for the subsequent coordination with dendrimers, and that a complex $PtCl_2(H_2O)_2$, which results from aquation, is the key species that gets coordinated with the tertiary amines in dendrimers. The coordination process is thus thought to be a consecutive reaction composed of two steps: the aquation of platinum ions and the coordination with dendrimers. On the basis of these findings, we then proposed a simple coordination scheme and calculated the coordination rate. The calculation results agreed well with the experimental results. The consecutive reaction mechanism qualitatively explains the experimental results of other metal species, in which metal ions with slower aquation rates require longer periods to get coordinated with dendrimers. Since rate constants are principally obtained from appropriate experimental analyses, we believe that our simple model is applicable to many types of metal ions and will help to describe the rate process of coordination, which is quite useful for optimizing the conditions required for effective nanoparticle synthesis.

■ ASSOCIATED CONTENT

Supporting Information. Absorbance difference at 250 nm of 5 μM [G4-OH + x Pt^{2+}] solutions during coordination process for 10 days, time-dependent UV−vis spectroscopic data obtained after mixing a 2 M NaCl solution and a 10 μM [G4-OH + 40 Pt^{2+}] solution, where Pt^{2+} coordination occurred completely, in equal amount, and time course of absorbance difference at 250 nm during Pt^{2+} coordination in G4-OH and G6-OH. This material is available free of charge via the Internet at http://pubs.acs.org.

■ AUTHOR INFORMATION

Corresponding Author
*E-mail: miyahara@cheme.kyoto-u.ac.jp.

■ ACKNOWLEDGMENT

This work was partly supported by the Grant-in-Aid for Scientific Research (B), Global Centers of Excellence (G-COE) program, and the Core-to-Core (CTC) Program from the Japan Society for the promotion of Science (JSPS).

■ REFERENCES

(1) Tomalia, D. A.; Baker, H.; Dewald, J.; Hall, M.; Kallos, G.; Martin, S.; Roeck, J.; Ryder, J.; Smith, P. A new class of polymers—Starburst-dendritic macromolecules. *Polym. J.* **1985**, *17*, 117–132.

(2) Matthews, O. A.; Shipway, A. N.; Stoddart, J. F. Dendrimers—Branching out from curiosities into new technologies. *Prog. Polym. Sci.* **1998**, *23*, 1–56.

(3) Zhao, M. Q.; Sun, L.; Crooks, R. M. Preparation of Cu nanoclusters within dendrimer templates. *J. Am. Chem. Soc.* **1998**, *120*, 4877–4878.

(4) Balogh, L.; Tomalia, D. A. Poly(amidoamine) dendrimer-templated nanocomposites. 1. Synthesis of zerovalent copper nanoclusters. *J. Am. Chem. Soc.* **1998**, *120*, 7355–7356.

(5) Zhao, M. Q.; Crooks, R. M. Dendrimer-encapsulated Pt nanoparticles: Synthesis, characterization, and applications to catalysis. *Adv. Mater.* **1999**, *11*, 217–220.

(6) Scott, R. W. J.; Wilson, O. M.; Crooks, R. M. Synthesis, characterization, and applications of dendrimer-encapsulated nanoparticles. *J. Phys. Chem. B* **2005**, *109*, 692–704.

(7) Kim, Y. G.; Oh, S. K.; Crooks, R. M. Preparation and characterization of 1−2 nm dendrimer-encapsulated gold nanoparticles having very narrow size distributions. *Chem. Mater.* **2004**, *16*, 167–172.

(8) Yamamoto, K.; Imaoka, T.; Chun, W. J.; Enoki, O.; Katoh, H.; Takenaga, M.; Sonoi, A. Size-specific catalytic activity of platinum clusters enhances oxygen reduction reactions. *Nat. Chem.* **2009**, *1*, 397–402.

(9) Niu, Y. H.; Yeung, L. K.; Crooks, R. M. Size-selective hydrogenation of olefins by dendrimer-encapsulated palladium nanoparticles. *J. Am. Chem. Soc.* **2001**, *123*, 6840–6846.

(10) Yamamoto, D.; Watanabe, S.; Miyahara, M. T. Coordination and reduction processes in the synthesis of dendrimer-encapsulated Pt nanoparticles. *Langmuir* **2009**, *26*, 2339–2345.

(11) Knecht, M. R.; Garcia-Martinez, J. C.; Crooks, R. M. Synthesis, characterization, and magnetic properties of dendrimer-encapsulated nickel nanoparticles containing <150 atoms. *Chem. Mater.* **2006**, *18*, 5039–5044.

(12) Oh, S. K.; Kim, Y. G.; Ye, H. C.; Crooks, R. M. Synthesis, characterization, and surface immobilization of metal nanoparticles encapsulated within bifunctionalized dendrimers. *Langmuir* **2003**, *19*, 10420–10425.

(13) Scott, R. W. J.; Ye, H. C.; Henriquez, R. R.; Crooks, R. M. Synthesis, characterization, and stability of dendrimer-encapsulated palladium nanoparticles. *Chem. Mater.* **2003**, *15*, 3873–3878.

(14) Esumi, K.; Nakamura, R.; Suzuki, A.; Torigoe, K. Preparation of platinum nanoparticles in ethyl acetate in the presence of poly(amidoamine) dendrimers with a methyl ester terminal group. *Langmuir* **2000**, *16*, 7842–7846.

(15) Gu, Y. L.; Xie, H.; Gao, J. X.; Liu, D. X.; Williams, C. T.; Murphy, C. J.; Ploehn, H. J. AFM characterization of dendrimer-stabilized platinum nanoparticles. *Langmuir* **2005**, *21*, 3122–3131.

(16) Tarazona-Vasquez, F.; Balbuena, P. B. Pt(II) uptake by dendrimer outer pockets: 2. Solvent-mediated complexation. *J. Phys. Chem. B* **2008**, *112*, 4182–4193.

(17) Tarazona-Vasquez, F.; Balbuena, P. B. Pt(II) uptake by dendrimer outer pockets: 1. Solventless ligand exchange reaction. *J. Phys. Chem. B* **2008**, *112*, 4172–4181.

(18) Tarazona-Vasquez, F.; Balbuena, P. B. Dendrimer-tetrachloroplatinate precursor interactions. 1. Hydration of Pt(II) species and PAMAM outer pockets. *J. Phys. Chem. A* **2007**, *111*, 932–944.

(19) Tarazona-Vasquez, F.; Balbuena, P. B. Dendrimer-tetrachloroplatinate precursor interactions. 2. Noncovalent binding in PAMAM outer pockets. *J. Phys. Chem. A* **2007**, *111*, 945–953.

(20) Zhou, L.; Russell, D. H.; Zhao, M. Q.; Crooks, R. M. Characterization of poly(amidoamine) dendrimers and their complexes with Cu^{2+} by matrix-assisted laser desorption ionization mass spectrometry. *Macromolecules* **2001**, *34*, 3567–3573.

(21) Gu, Y. L.; Sanders, P.; Ploehn, H. J. Quantitative analysis of Pt-PAMAM ligand exchange reactions: Time and concentration effects. *Colloid Surf. A* **2010**, *356*, 10–15.

(22) Knecht, M. R.; Weir, M. G.; Myers, V. S.; Pyrz, W. D.; Ye, H. C.; Petkov, V.; Buttrey, D. J.; Frenkel, A. I.; Crooks, R. M. Synthesis and characterization of Pt dendrimer-encapsulated nanoparticles: Effect of the template on nanoparticle formation. *Chem. Mater.* **2008**, *20* 5218–5228.

(23) Crooks, R. M.; Zhao, M. Q.; Sun, L.; Chechik, V.; Yeung, L. K. Dendrimer-encapsulated metal nanoparticles: Synthesis, characterization, and applications to catalysis. *Acc. Chem. Res.* **2001**, *34*, 181–190.

(24) Grantham, L. F.; Elleman, T. S.; Martin, D. S. Exchange of chlorine in aqueous systems containing chloride and tetrachloroplatinate(II). *J. Am. Chem. Soc.* **1955**, *77*, 2965–2971.

(25) Elding, L. I.; Olsson, L. F. Electronic absorption-spectra of square-planar chloro-aqua and bromo-aqua complexes of palladium(II) and platinum(II). *J. Phys. Chem.* **1978**, *82*, 69–74.

(26) Elding, L. I. Stepwise dissociation of tetrachloroplatinate(II) ion in aqueous solution. 6. rates of formation and equilibria of chloro aqua complexes of platinum(II). *Acta Chem. Scand.* **1970**, *24*, 1527–1540.

(27) Elding, L. I.; Leden, I. On stepwise dissociation of tetrachloridoplatinate(2) ion in aqueous solution. 1. equilibria at 25degreec. *Acta Chem. Scand.* **1966**, *20*, 706–715.

(28) Pellechia, P. J.; Gao, J. X.; Gu, Y. L.; Ploehn, H. J.; Murphy, C. J. Platinum ion uptake by dendrimers: An NMR and AFM study. *Inorg. Chem.* **2004**, *43*, 1421–1428.

(29) Reedijk, J. Metal-Ligand Exchange Kinetics in Platinum and Ruthenium Complexes significance for effectiveness as anticancer drugs. *Platinum Met. Rev.* **2008**, *52*, 2–11.

(30) Nepomnyashchii, A. B.; Alpuche-Aviles, M. A.; Pan, S. L.; Zhan, D. P.; Fan, F. R. F.; Bard, A. J. Cyclic voltammetry studies of Cd^{2+} and Zn^{2+} complexation with hydroxyl-terminated polyamidoamine generation 2 dendrimer at a mercury microelectrode. *J. Electroanal. Chem.* **2008**, *621*, 286–296.

(31) Jesus, Y.; Vicente, A.; Lafaye, G.; Marecot, P.; Williams, C. T. Synthesis and characterization of dendrimer-derived supported iridium catalysts. *J. Phys. Chem. C* **2008**, *112*, 13837–13845.

(32) Ye, H. C.; Crooks, R. M. Electrocatalytic O-2 reduction at glassy carbon electrodes modified with dendrimer-encapsulated Pt nanoparticles. *J. Am. Chem. Soc.* **2005**, *127*, 4930–4934.

(33) Lafaye, G.; Williams, C. T.; Amiridis, M. D. Synthesis and microscopic characterization of dendrimer-derived Ru/Al_2O_3 catalysts. *Catal. Lett.* **2004**, *96*, 43–47.